Modeling impacts of climate change on the water needs and growing cycle of crops in three Mediterranean basins.

Funes I.[1*], Savé R.[1], de Herralde F.[1], Biel C.[1], Pla E.[2], Pascual D.[2], Zabalza J.[3], Cantos G.[4], Borràs G.[4], Vayreda J.[2] & Aranda X.[1]

[1] IRTA (Institute of Agrifood Research and Technology), Torre Marimon, Caldes de Montbui (Barcelona), Spain

[2] CREAF, Centre de Recerca Ecològica i Aplicacions Forestals, E-08193 Bellaterra (Cerdanyola del Vallès), Spain

[3] IPE-CSIC (Pyrenean Institute of Ecology), Estación Experimental de Aula Dei - CSIC, Zaragoza., Spain

[4] OCCC (Catalan Office for Climate Change. Government of Catalonia), Avinguda Diagonal, 523-525, 08029 Barcelona, Spain.

Abstract

In this study, the suitability of major crops currently growing in three case study basins in Catalonia (NE Spain) was assessed for the first half of the 21st century. For this purpose, an estimation was made of net hydric needs (NHN) and a set of agroclimatic parameters. Climate change impacts were estimated at sub-basin level using temperature and precipitation temporal series based on the Third Report on Climate Change in Catalonia under the RCP4.5 scenario. Potential crop evapotranspiration (ETc, FAO procedure) and monthly water balance considering soil water holding capacity were used to estimate actual evapotranspiration (ETa) and NHN. Over the period studied, NHN would generally rise , with small (+0.1%) to high (+6.6%) increases in the 2020s and moderate

(+3.9%) to high (+6.7%) increases in the 2040s. Dynamics would be different for the three basins and general trends vary from crop to crop. At all events, a generalized increase in NHN together with lower water availability could severely limit crop productivity in the case of both rainfed and irrigated crops (irrigation restrictions). Phenological changes could represent a greater constraint for crop productivity. Overall, the number of frost days will decrease (from -0.1 days in March to -8.7 days in April) in the three basins, while extremely hot days will increase (from +0.3 days in July to +3.8 days in August). Growth cycles will begin earlier (from -1 days to -12 days for crops with a base temperature of 10 ºC), and for some crops they will be shorter (from -8 days to -27 days in the case of maize and up to -10 days in the case of vines). The impacts of climate change in the three basins could result in significant limitations for crops if adaptive strategies beyond irrigation and growing cycle issues are not applied. The results of this study could serve as a basis for the development of adaptation strategies to improve and maintain agriculture in the case study basins and in similar regions.

Keywords

Watershed; Agriculture; Net hydric needs; Crop phenology; Adaptation

Highlights

- The main impacts of climate change on crops until 2050 was assessed in three Mediterranean basins.
- Modeling was performed at sub-basin level under the RCP4.5 scenario.
- Net hydric needs of crops are expected to increase (from +0.1% to +6.7%) in all basins.
- Advancement (1-12 days) and shortening (8-27 days) of the growing cycle are expected.
- A baseline to design adaptation and mitigation strategies was drawn.

***Corresponding author.** Full permanent address: IRTA Torre Marimon, C-59 km 12.1, 08140 Caldes de Montbui, Barcelona (Spain). Tel.: +34 902 789 449; E-mail address: inmaculada.funes@irta.cat

1. Introduction

In future climate change (CC) scenarios, the Mediterranean region stands out as a “hot spot” due to projections of substancial increases in temperature and decreases in rainfall (IPCC, 2014), which would lead to marked decreases in water availability throughout the Mediterranean region (Pascual et al., 2015). For example, in Catalonia (NE Spain) average annual precipitation would decrease by approximately 9% and temperature would increase by +1.4 ºC until 2050 (TICCC, 2016). Agriculture is and will continue to be one of the systems most affected by CC, since – alongside radiation – temperature and water are the main drivers of crop production (Phogat et al., 2018; Ruiz-Ramos et al., 2018). In the Mediterranean region, agriculture is expected to be heavily impacted by higher and extreme temperatures, droughts or soil salinity. To be specific, the principal CC impacts on crops would be changes in phenology and growing cycle (Trnka et al., 2011; Caubel et al., 2015; Funes et al., 2016); higher water demands (Savé et al., 2012; Girard et al., 2015; Phogat et al., 2018; Saadi et al., 2015; Valverde et al., 2015; Zhao et al., 2015) and water scarcity (Vicente-Serrano et al., 2017a,b); decreasing yields (Olesen and Bindi, 2002; Saadi et al., 2015; Zhao et al., 2015; Ruiz-Ramos et al., 2018); or soil salinity constraints (Connor et al., 2012; Phogat et al. 2018). Consequently, food production and security would be seriously compromised (Cramer et al., 2018).

Assessing how climate is expected to affect crops is extremely useful for policy makers, planners, farmers and other stakeholders, who can propose and execute adaptation and mitigation strategies at the local/regional scale to make agriculture more resilient to changes (Caubel et al., 2015). The use of combined adaptation measures tailored to site-specific conditions reduces the impacts of CC more effectively than single and generalized adaptation measures: this has been shown by Ruiz-Ramos et al. (2018) for the Mediterranean context, but can probably be applied to other regions. In general, both adaptation and mitigation strategies have to be addressed in order to reduce greenhouse gas emissions (GHGs), sequester carbon, protect crops from extreme events and ensure sustainable use of soil and water (Prestele et al., 2018). Indeed, climate-smart agriculture (FAO, 2013) has been proposed by FAO as a strategy to adapt and build resilience to CC and to reduce agricultural GHGs, while maintaining high yields and ensuring food security. In summary, strategies and policies must consider productivity, adaptation and mitigation as the three interlinked pillars that support the successful achievement of targeted goals for agriculture and CC issues (FAO, 2013). Therefore, when seeking to identify better strategies to make agriculture more resilient, the first step is to assess the main impacts of CC on crops.

Future water availability and water demands call the current water management model into question, so adaptation decisions must necessarily be aimed at improving water management at a policy level (Iglesias and Garrote, 2015) and target both hazards and vulnerabilities, i.e. water supply and water demand issues (Ronco et al., 2017). Changes in crop distribution and crop choices (Valverde et al., 2015), restricting areas of higher water-consuming crops or creating new varieties adapted to CC (Mo et al., 2017), adapting the cropping calendar (Ronco et al., 2017) and crop diversification (Lin, 2011) have all been proposed as strategies of adaptation to CC for the purpose of maintaining crop production. But they should also be considered as part of a water management strategy: restricting the area of high-consuming crops, even if they are not irrigated, will free water resources at the basin level; changing crop distributions according to changes in phenological constraints, reducing the crop cycle and using new varieties with lower water needs would be steps in the same direction.

This study forms part of the LIFE MEDACC Project (LIFE12 ENV/ES/000536 Demonstration and validation of innovative methodology for regional climate change adaptation in the Mediterranean area). One of the main objectives of this project is assessment of the impacts of climate on agriculture, forest and water at the basin level. Ecohydrology served as a central tool, as it allows consideration of human interference on water balance at the landscape level by using the river basin as a geo-hydrological unit (Savé et al., 2012). The basin has been an appropriate natural unit for assessing or planning any initiative or strategy aimed at conservation, regeneration, adaptation or mitigation to CC. Catalonia is suitably representative of the Mediterranean region, since it presents a wide range of climate conditions in a relatively small area (Pascual et al., 2015).

In this study, three basins were chosen to represent the diversity of the Mediterranean at a local scale. They feature a wide range of topographic, climatic and environmental conditions, and land uses of the Mediterranean region, particularly of Catalonia, including inland vs. coastal differences, which makes this study novel. Another novel feature of this study is that this is the first time an improved upscaling of net hydric needs (NHN) has been applied to these three sub-basins. The improved upscaling uses homogeneous climate, crop type and soil type units. This leads to an understanding of how changes in basin water balance result from the combination of changes in crop phenology, potential evapotranspiration and crop distribution in each basin. This approach worked well in previous studies (Savé et al., 2012), showing CC effects such as increased net water needs and changes in phenology and crop growing cycle (Savé et al., 2012), or impacts on apple flowering time (Funes et al., 2016), despite the fact that in those studies AR4 scenarios A1 and B2 were used instead of RCPs of AR5 (IPCC 2014), a different methodology for projections was employed, results were only obtained for a single coastal basin, and the most notable results corresponded to the second half of the 21st century, a period not considered here.

The main goals of this study were: (i) to estimate annual net hydric needs (NHN) of major crops in the three basins for the baseline period and two future periods under CC conditions, in order to assess agricultural suitability; (ii) to estimate the monthly pattern of NHN of some crops, which helps to explain the different annual NHN responses of crops to CC; (iii) to estimate a set of agroclimatic parameters capable of indicating the consequences of CC for crop phenology and growing cycle, in order to better understand and manage the risks posed by CC; and (iv) to identify a set of possible adaptation solutions, in view of the results obtained.

2. Material and Methods

A general overview of the material and methods is shown in Figure 1.

2.1. Study area

The study area comprises three basins: those of the river Segre, Ter and Muga. The basins are located in Catalonia (NE Spain; Fig. 2) under Mediterranean conditions, with an area of 13,205, 2,952 and 762 km^2 respectively. These basins were chosen to represent the diversity of the Mediterranean region at a local scale, with a wide range of topographic, climatic and environmental conditions (Pyrenean, inland and coastal; Fig. A.1 of Appendix A), and land uses (Table 1).

The Segre is the longest river in Catalonia (it is a tributary of the Ebro River). The Segre basin is highly stressed by agricultural demands (it is the most agricultural and irrigated basin; Table 1). Water demand in the Ter basin is mainly for urban users (74% in 2007) inside and outside the basin, and as a result, the ecological flows defined for the lower part of the river

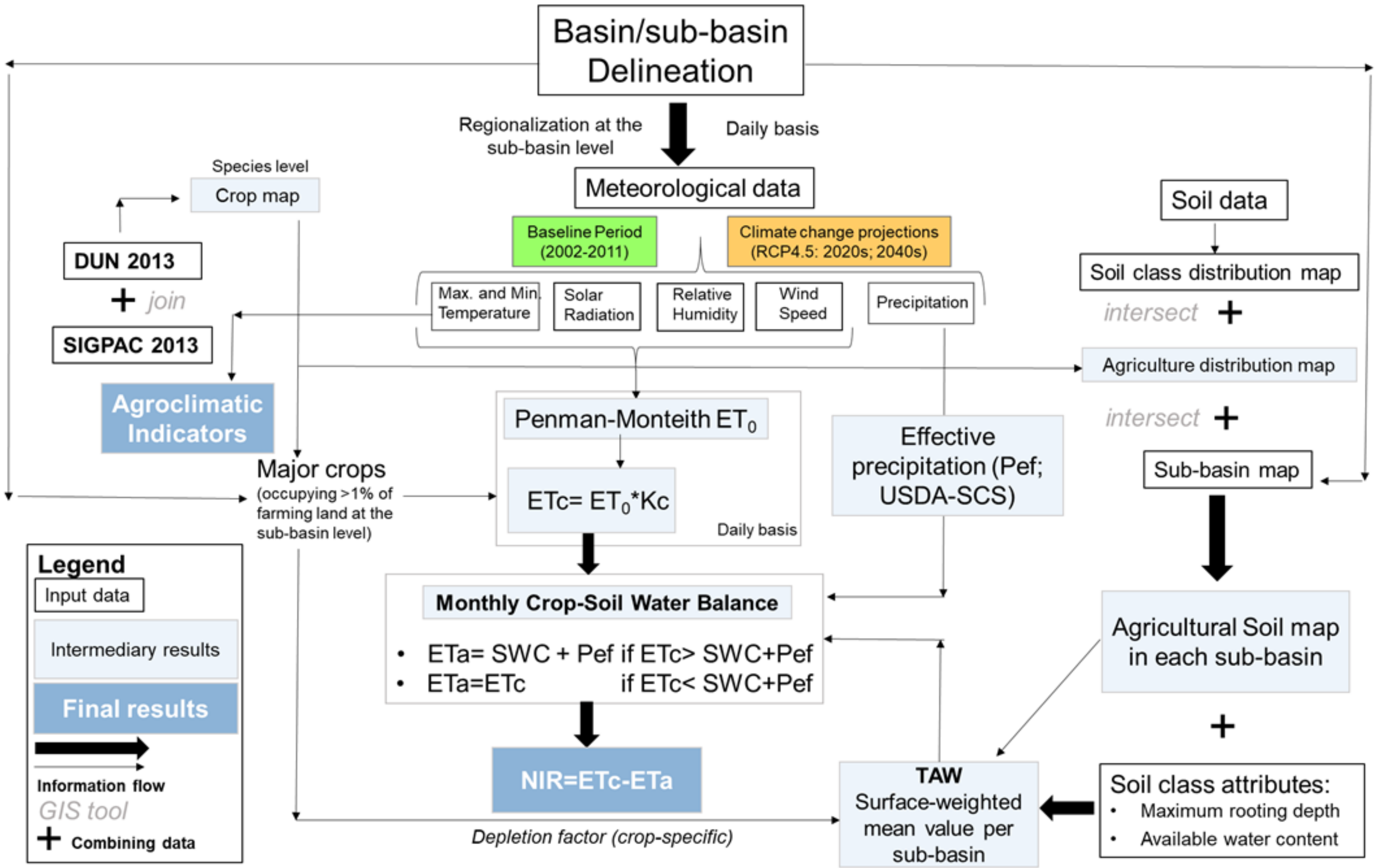

Figure 1. General overview of *Material and Methods*. ET_0 is potential evapotranspiration, ETc is crop evapotranspiration, Kc is crop coefficient, ETa is actual evapotranspiration, SWC is soil water content, Pef is effective precipitation, TAW is total available water and NHN is net hydric needs

are frequently not achieved. Moreover, the Ter basin is densely forested. The Muga basin is strongly influenced by its coastal condition. Crops obtain 75% of its water, whereas urban users receive 20%.

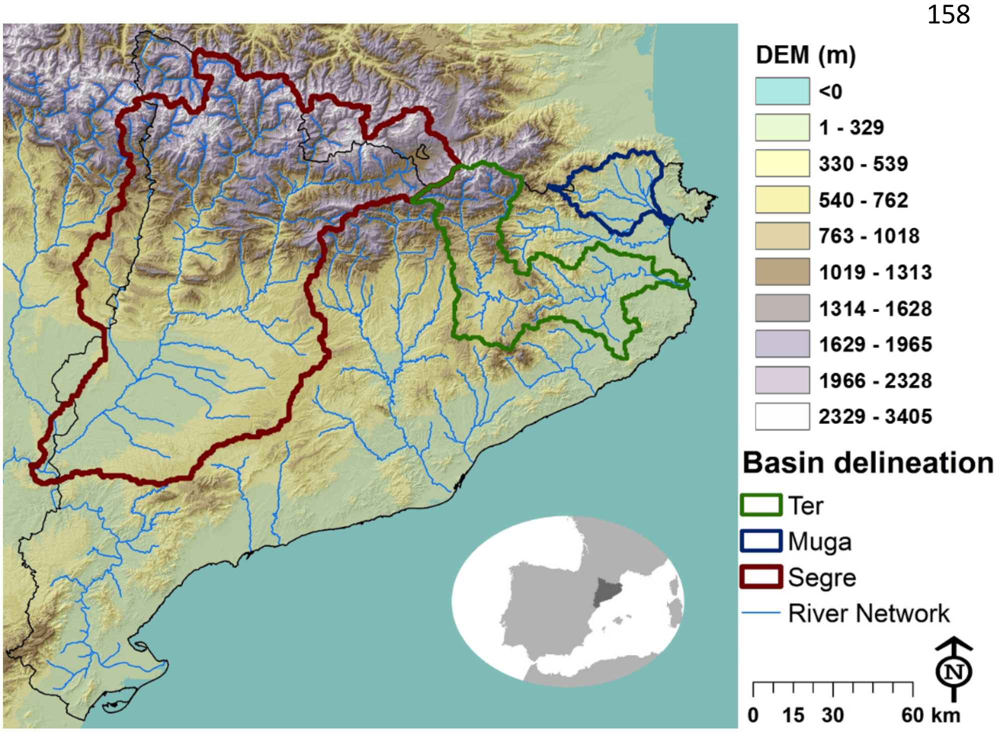

Figure 2. Location of the case study basins. The digital elevation model (DEM) represents altitude (above sea level) in the study area.

Table 1. Areas of major crops and other land uses within the case study basins delineated by SWAT, and percentage of irrigated land for each crop according to the agricultural plots geographical information system (SIGPAC, 2013), the declaration of eligible agricultural area for Common Agricultural Policy payments of the Government of Catalonia (DUN, 2013), and other data sources outside Catalonia (Aragon, France and Andorra). Numbers in brackets are percentages of each land use with respect to the whole basin area.

Land use		Area (ha)			% irrigated		
		Segre	Ter	Muga	Segre	Ter	Muga
Crops	Winter cereals	185,306	27,011	7,730	16	16	24
	Maize	32,112	5,463	1,912	98	62	90
	Forage crops	40,327	13,437	3,344	66	12	26
	Other Arable land	10,168	4,618	1768	33	18	30
	Orchards	42,863	1,719	449	96	90	53
	Olives	38,770	237	1,473	11	8	1
	Nuts	16,563	879	40	12	50	31
	Vineyards	3,842	72	895	37	5	4
	Tree Farming	85	1,235	-	92	1	-
	Total Crops	**369,950 (28%)**	**54,671 (19%)**	**17,611 (23%)**	38	22	30
	Forest	**296,337 (22%)**	**112,125 (38%)**	**31,421 (41%)**			
	Grassland	**557,712 (42%)**	**103,710 (35%)**	**21,875 (29%)**			
	Urban	**50,781 (4%)**	**15,040 (5%)**	**4,473 (6%)**			

Major crops are considered to be those occupying more than 1% of the crop area at the sub-basin level. Winter cereals comprise wheat, barley, oats and triticale. The group of forage crops is composed of alfalfa, ryegrass, artificial meadows, polyphytic pastures and other forage crops. Other arable land consists of oleaginous crops, cereals and horticulture. Orchards refer to plantations of sweet fruit trees. Nuts are almonds, walnuts, hazelnuts and pistachio trees. Grassland refers to pastures, woodland pastures and bush pastures (all three SIGPAC land uses). Tree farming refers to poplar plantations.

2.2. Basin delineation, climate change projections and meteorological parameter regionalization at the sub-basin level.

Basin and sub-basin delineation was performed using SWAT (Soil and Water Assessment Tool; Arnold et al., 1998) and based on a digital elevation model of 30 m resolution (ICC, 2012). Sub-basin delimitation was based on elevation, creating units with similar areas (Fig. A.2 of Appendix A).

Daily meteorological data were obtained from 340 stations managed by the Spanish State Meteorological Agency (AEMET) and the Meteorological Service of Catalonia (SMC). Some of the meteorological stations also provided data on radiation, relative humidity and wind speed (see spatial distribution of weather stations in Fig. A.3 of Appendix A). The stations were chosen according to their locations within or close to the case study basins, considering climatic heterogeneity and continuity in data series. Climate data were subjected to a process of quality control, filling gaps and homogenization. More detailed information about climate data processing can be found in Appendix B.

CC projections for temperature and precipitation were conducted using the RCP4.5 scenario (IPCC, 2014) until the time horizon 2050. The RCP4.5 scenario is a stabilization scenario in which total radiative forcing is stabilized shortly after 2100, without overshooting the long-run radiative forcing target level (Pascual et al., 2016). The time horizon of 2050 was chosen, because short temporal periods are more appropriate for territorial policies in the study area (land planning, irrigation plans, etc.). This may make it difficult to see clear changes from the baseline, but on the other hand the capacity of long temporal time frames to predict reliable changes is limited.

The future temporal series are based on information in the Third Report on Climate Change in Catalonia (TICCC) about the regional dynamic downscaling of CORDEX/EUROCORDEX climate change projections for the three main climatic sub-regions in Catalonia: Pyrenees, Inland and Coast (TICCC, 2016). The changes in temperature and precipitation proposed in TICCC (TICCC, 2016) were applied to the observed temperature and precipitation series of the meteorological stations (those in or near the case study basins) for the baseline period (2002-2011), year by year, at the daily scale, by using the delta method (Zahn and Storch, 2010). A different delta was applied to each month of the year, in accordance with the results of TICCC (2016).

To estimate potential evapotranspiration (ET_0) according to Penman-Monteith, meteorological parameters needed (such as solar radiation, humidity and wind speed) were estimated at a daily scale by using the weather generator included in SWAT (Neitsch et al., 2005). This uses statistics, based on measured records of each weather station, to complete missing information or simulate representative daily climatic data for the sub-basin. More details of these statistics are explained in Neitsch et al. (2011).

Moreover, SWAT was employed to regionalize the meteorological parameter series at the sub-basin scale to be used in the remainder modeling. More details about meteorological parameter regionalization at the sub-basin level can be found in Appendix B.

Taking into account the changes presented in TICCC, the plausible scenario for the study area is a general warming (Table 2 and Fig. A.4) in all the basin segments and in both temporal horizons analyzed (from +0.6 ºC to +1.3 ºC), leading to a general increase in ET_0 (from +2.0% to +4.7%). Projections show higher warming in the sub-regions Pyrenees and Inland than in Coast. As for precipitation, a decrease is likely (between -3.7% and -14.2%; Table 2 and Fig. A.4), but with lower certainty (TICCC, 2016).

Table 2. Overview of the spatial distribution at the sub-basin level of: a) mean annual precipitation (MAP; mm); b) mean annual evapotranspiration (ET_0; mm) and c) mean annual temperature (MAT; ºC) in the three case study basin segments for the baseline period (2002-2011) and differences in % (MAP and ET0) or ºC (MAT) for both future decades analyzed under the RCP 4.5 scenario: 2020s (2021-2030) and 2040s (2041-2050).

		Segre			Ter			Muga		
	Basin Segment	Baseline (mm)	2020s (Δ %)	2040s (Δ %)	Baseline (mm)	2020s (Δ %)	2040s (Δ %)	Baseline (mm)	2020s (Δ %)	2040s (Δ %)
MAP	Upper	**932**	+0.1	-1.4	**981**	-7.5	-8.9	**1045**	-3.7	-10.0
	Middle	**755**	-14.1	-14.2	**876**	-8.5	-11.3	**811**	-5.7	-11.7
	Lower	**403**	-9.3	-10.1	**760**	-8.7	-12.8	**674**	-7.1	-12.2
ET_0	Upper	**419**	+2.6	+3.5	**805**	+2.7	+4.5	**816**	+2.5	+3.8
	Middle	**907**	+3.7	+4.7	**892**	+2.0	+3.7	**853**	+2.3	+3.3
	Lower	**979**	+3.4	+4.4	**928**	+1.5	+3.1	**870**	+2.1	+3.1
		Baseline (ºC)	2020s (Δ ºC)	2040s (Δ ºC)	Baseline (ºC)	2020s (Δ ºC)	2040s (Δ ºC)	Baseline (ºC)	2020s (Δ ºC)	2040s (Δ ºC)
MAT	Upper	**7.3**	+0.7	+1.2	**9.7**	+0.9	+1.3	**12.6**	+0.60	+1.1
	Middle	**11.8**	+0.7	+1.2	**13.1**	+0.7	+1.1	**14.7**	+0.60	+1.0
	Lower	**14.4**	+0.8	+1.2	**14.7**	+0.6	+1.0	**15.4**	+0.66	+1.0

2.3. Agricultural land uses

A crop distribution map at species level was created for each basin from SIGPAC and DUN for the year 2013 (map scale 1:5,000). Methodological details about the crop mapping can be found in Appendix B.

Most crops in the Segre basin occupy the lower basin and tend to be grouped according to crop typology. The main crops in this lower basin are rainfed winter cereals (Table 1), located mainly in the eastern part of the lower basin and even extending to the middle basin (Fig. 3). The central part of the lower basin (Lleida Valley) is dominated by maize, fruit orchards and alfalfa. In the western part of the lower basin, the agricultural land is primarily occupied by nectarine or peach trees. There are some important areas of grape production, and olives and almonds are grown in the southern part. The lower and middle parts of the Ter basin are devoted to agriculture (Fig. 3). Two crops dominate the lowest part of the lower Ter: apple and maize, which are in fact the two most irrigated crops in the basin (Table 1).

Herbaceous crops such as winter cereals, sorghum, sunflower, rape, etc. and some woody crops such as hazel occupy the remainder of the lower Ter. In the middle Ter, herbaceous crops such as winter cereals, maize, sorghum, rape and fodder crops predominate. Crops in the Muga basin occupy the middle and lower segments (Fig.3). Maize is commonly found in the lower part, while winter cereals are widespread in the lower and middle basin segments. Fodder and woody crops, such as olives and vines (mostly rainfed; Table 1), dominate the middle part of the basin. The irrigated land in this basin is mainly occupied by maize and alfalfa or fruit orchards, such as apple or peach (Table 1). Winter cereals are mostly rainfed, except wheat in the lower basin, with an irrigated area of as much as 43% (Table 1).

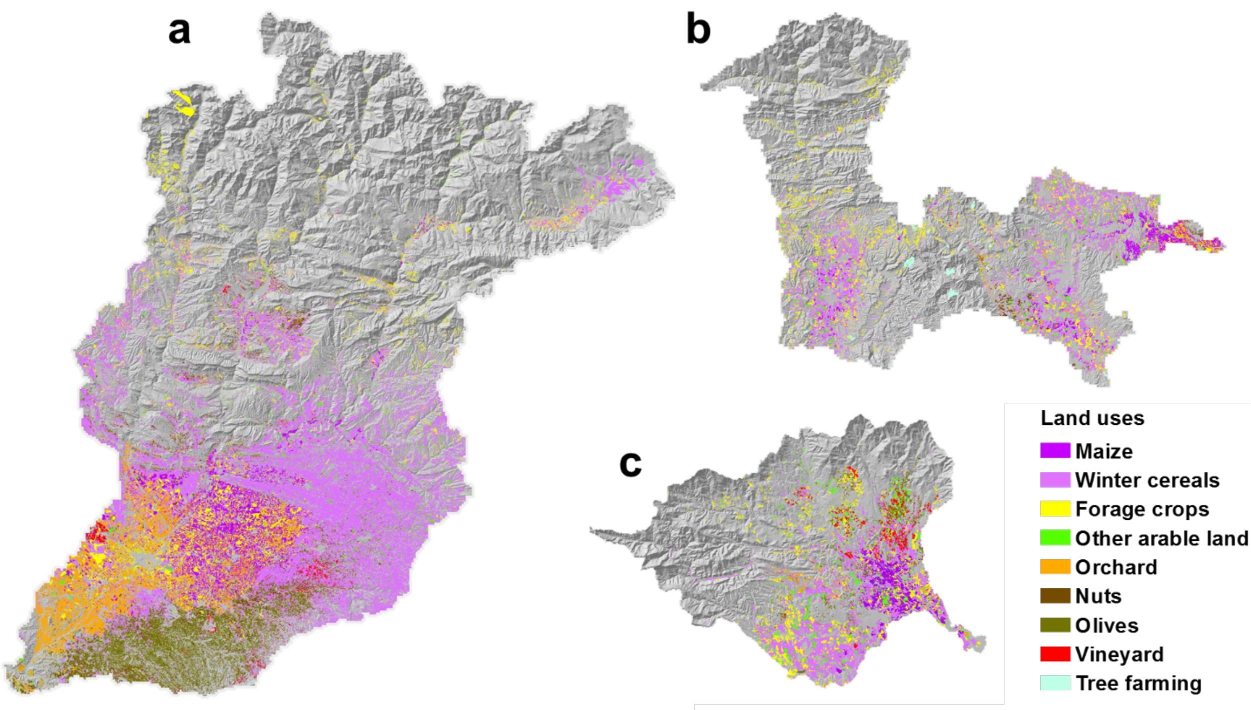

Figure 3. Agricultural land use distribution in the case study basins (a) Segre, b) Ter and c) Muga according to SIGPAC 2013 and DUN 2013 for Catalonia and other regional and national sources for areas beyond Catalonia. A description of land uses in this figure can be found in the footnotes to Table 1. Grayscale hillshading represents topography of non-agricultural areas.

2.4. Available water capacity of agricultural soils

Soil maps were specifically generated for the three basins (map resolution 100x100 m), since they were not previously available for these basins at an appropriate resolution. Details about soil mapping methodology can be found in Appendix B. For each basin, the resulting soil map was intersected with the sub-basin map and the crop map in order to calculate the area of each soil class corresponding to the agricultural land in each sub-basin. In this way, it was possible to estimate an area-weighted mean value in each sub-basin for the following soil attributes: maximum rooting depth of soil profile (Z; mm) and available water capacity of the soil layer (AWC; mm H_2O/mm soil). AWC was calculated by subtracting the fraction of water present at permanent wilting point (the soil water content at a soil matric potential of -1.5 MPa) from that present at field capacity (the soil water content at a soil matric potential of -0.033 MPa) (Neitsch et al., 2011). By multiplying both values (Z and AWC) at sub-basin level, a mean value of a maximum soil water capacity was obtained that could subsequently be used in NHN estimations as the Total Available Soil Water (TAW; mm).

For all three basins, soils were classified into 5 TAW classes (Table 3 and Fig. A.5 in Appendix A). In the Muga basin, cropland mainly corresponds to soils with the two highest TAW classes (ranging from 150 to 300 mm), since the best soils, those with the highest capacity to store water, are sought for agricultural activity. In the Ter basin, crops are grown in the three highest classes of soil (ranging from 100 to 300 mm). However, in the Middle Ter the soils used for agriculture have a lower TAW classification (100-150 mm). In the Segre basin, agricultural land is largely situated in the lower Segre, irrespective of the capacity of soils to store water.Crops with higher water requirements such as maize, alfalfa and fruit orchards occupy the soils with the highest TAW values (200-300 mm), leaving the soils with lower TAW values (<150 mm) to crops such as winter cereals and woody crops such as olives or almonds.

Table 3. Areas (ha) of the total available soil water (TAW) classes in the whole basin and segments of the Segre, Ter and Muga basins. The numbers in brackets are percentages representing the proportion of the total agricultural area occupied by each class.

TAW (mm)	ha (%)											
	Segre				Ter				Muga			
	Total Basin	Upper	Middle	Lower	Total Basin	Upper	Middle	Lower	Total Basin	Upper	Middle	Lower
15-30	**96,663 (24.5)**	2,365 (11.4)	16,636 (19.0)	77,662 (27.1)	**2,081 (3.8)**	329 (8.5)	651 (3.2)	1,102 (3.7)	**189 (1.3)**	19 (10.4)	49 (0.9)	120 (1.3)
30-100	**136,245 (34.5)**	1,771 (8.5)	38,509 (44.0)	95,965 (33.5)	**6,107 (11.3)**	1,389 (35.9)	4,071 (19.8)	647 (2.2)	**1,688 (11.2)**	126 (68.3)	654 (11.9)	907 (9.7)
100-150	**47,306 (12.0)**	10,580 (51.0)	18,297 (20.9)	18,429 (6.4)	**22,889 (42.2)**	1,685 (43.6)	13,400 (65.3)	7,805 (26.1)	**1,654 (11.0)**	30 (16.1)	1,281 (23.3)	344 (3.7)
150-200	**13,888 (3.5)**	97 (0.5)	1,716 (2.0)	12,076 (4.2)	**9,985 (18.4)**	39 (1.0)	783 (3.8)	9,163 (30.6)	**8,400 (56.0)**	3 (1.6)	2,332 (42.4)	6,065 (65.1)
200-300	**101,044 (25.6)**	5,950 (28.7)	12,338 (14.1)	82,756 (28.8)	**13,220 (24.4)**	426 (11.0)	1,615 (7.9)	11,179 (37.4)	**3,075 (20.5)**	7 (3.7)	1,186 (21.6)	1,882 (20.2)

2.5. Net hydric needs estimations

Daily crop potential evapotranspiration (ETc, mm day^{-1}) was calculated for major crops (those occupying more than 1% of the crop area at sub-basin level) in the three basins according to FAO procedure in Allen et al. (1998). ET_0 was calculated from the meteorological series regionalized at the sub-basin level by SWAT from 2002 to 2050. First, daily potential evapotranspiration (ET_0, mm day^{-1}) was calculated in the usual way by applying the Penman-Monteith equation, which is the most appropriate for a Mediterranean climate of all the methods available in SWAT for potential evapotranspiration estimation (Licciardello et al., 2011). Secondly, ETc was calculated for each major crop in each sub-basin from the general ET_0 of the sub-basin and a crop coefficient (Kc, dimensionless) modified by crop phenological stage, as follows:

$$ETc=ET_0\ Kc \qquad [1]$$

Since the reference surface considered for ET_0 is a hypothetical grass reference crop that resembles an extensive surface of green, well-watered grass of uniform height, actively growing and completely shading the ground (Allen et al., 1998), ETc of grassland and other herbaceous crops such as ryegrass were considered to be equal to ET_0 (Kc=1). In the case of alfalfa and olives, ETc was estimated using a fixed Kc value of 0.78 and 0.65, respectively. For the remaining major crops, Kc values were based on those published in ACA and IRTA (2008), a compilation of different studies estimating Kc coefficients for different crops in Catalonia (Girona et al., 2004, 2011, Marsal et al. 2013, 2016). Kc coefficients are defined in these publications following the crop growth function, based on accumulated growing degree days (GDD). For this study, GDD were adapted to different base temperatures depending on the crop typology. More details are described in Vicente-Serrano et al. (2014).

Under FAO procedure, ETc corresponds to the crop evapotranspiration under standard conditions. These standard conditions refer to crops grown in large fields under excellent agronomic and soil water conditions. However, ETc may actually be limited by available water coming from rain and soil water content. In this case, ETc is reduced to the so-called actual evapotranspiration (ETa, mm $month^{-1}$). Thus, for the land area occupied by each crop in each sub-basin, a monthly water balance was recurrently calculated to obtain ETa from ETc, effective precipitation (Pef, mm $month^{-1}$) and the soil water content (SWC, mm $month^{-1}$), as follows:

$$\text{if } ETc > SWC_{-1} + Pef; \quad \text{and} \quad \begin{cases} ETa = SWC_{-1} + Pef & [2] \\ SWC_C = 0 & [3] \end{cases}$$

$$\text{if } ETc < SWC_{-1} + Pef; \quad \begin{cases} ETa = ETc & [4] \\ \text{and} & \\ SWC_C = SWC_{-1} + Pef - ETa \quad \text{or} \quad SWC_C = RAW & [5] \end{cases}$$

where ETc, ETa and Pef are from the current month, SWC_{-1} is the surplus SWC at the end of the previous month and SWC_C is water remaining in the soil at the end of the current month and available for crop consumption in the water balance of the next month (i.e. SWC_C of current month equals SWC_{-1} of next month, and so on). RAW (readily available water, mm) is the amount of water that a crop can extract from the root zone without suffering water stress. RAW was calculated for each crop and sub-basin from Total Available Water for each basin (TAW, see section 2.4) and a depletion factor (p) for each crop:

$$RAW = p\ TAW \qquad [6]$$

Theoretically, p ranges from 0 to 1. A value of 0.50 for p is commonly used for many crops. For major crops in the case study basins, values for p in the range of 0.50-0.55 were quite common. The minimum value for p was 0.40, corresponding to almonds, and the maximum 0.65, corresponding to olives (Allen et al., 1998).

Hence, after RAW calculation, SWC surplus for the next month (SWC_C) is calculated as:

$$SWC_C = RAW \qquad \text{if } SWC_{-1} + Pef - ETa > RAW \qquad [7]$$

$$SWC_C = SWC + Pef - ETa \qquad \text{if } SWC_{-1} + Pef - ETa < RAW \qquad [8]$$

Pef in equations [2], [5], [7] and [8] was calculated according to Clarke (1998):

$$Pef = \begin{cases} Pef = \frac{Pt(125-0.2Pt)}{125}; \text{ (Pt<250mm)} & [9] \\ Pef = 125 + 0.1Pt; \text{ (Pt≥250mm)} & [10] \end{cases}$$

where Pt is the total monthly precipitation (mm).

Finally, net hydric needs of the crops (NHN, mm month^{-1}) at the monthly scale were calculated as the difference between ETc and ETa:

$$NHN=ETc-ETa \quad [11]$$

Calculated in this way, NHN does not take account of water inefficiencies in the irrigation system or water pipes used for distribution, i.e. only plant level water requirements are considered. Moreover, projections of NHN estimations in this study do not take into consideration possible changes in agricultural land use (crop changes, abandonment, afforestation, or conversion to urban or industrial soil) for the first half of the 21st century. Theoretical net hydric needs of major crops were calculated for both rainfed and irrigated cropland in each basin.

2.6. Phenological and agroclimatic indicators

Phenological and agroclimatic indicators were calculated to assess the suitability of present-day crops to conditions projected for the near future. A set of general agroclimatic indicators was calculated for the baseline period and the future period up to 2050 under the RCP4.5 CC scenario. Indicators affecting crops in general were estimated following Savé et al. (2012)

and are detailed in Table 4. In addition, some crop-specific indicators for maize, grapevine and apple were calculated.

Table 4. General and crop-specific phenological and agroclimatic indicators of climate change impacts on agriculture: definition, units, climatic parameter on which each indicator is based, and basin segment in which they were estimated. Tmax is the daily maximum temperature (ºC), Tmin is the daily minimum temperature (ºC), Tmean is the daily average temperature (ºC) and DOY is the day of year.

Crop	Climate impacts	Phenological/ Agroclimatic indicator	Definition	Units	Climatic parameter	Basin Segment
All major crops	Frost damage in germination of some cereals and flowering of woddy crops	*Frost days*	Number of days with minimum temperature lower than 0ºC in March and April	days	Tmin	All basins and segments
	Heat damage in blossom and grain formation of some cereals	*Heat 30 days*	Number of days with temperature higher than 30 ºC in July and August	days	Tmax	
	Heat damage/stress in orchard fruits	*Heat 35 days*	Number of days with temperature higher than 35 ºC in July and August	days	Tmax	
	Beginning of growing cycle of most of the crops	*DOY T10*	Day when daily mean temperature begins to be higher 10ºC	DOY	Tmean	
Maize	Duration of growing cycle	*DOY 600FAO*	Day when 2076 GDD (Tbase=10ºC) were reached from 1st January to assess the cycle duration of FAO cycle grain maize varieties of 600	days	Tmean	Lower Segre; Lower Ter; and middle and Lower Muga
	Duration of growing cycle	*DOY 700FAO*	Day when 2126 GDD (Tbase=10ºC) were reached from 1st January to assess the cycle duration of FAO cycle grain maize varieties of 700	days	Tmean	
Grapevine	Time and duration of phenological stages	*DOY pheno* *Days pheno*	Date when grapevine budbreak, flowering, fruitset, pea size, veraison and harvest stages are completed[a] Days passing between phenological stages[a]	DOY days	Tmean	Lower Segre
Apple	Time of phenological stages	*DOY bloom*	Date when apple flowering is completed in 8 apple cultivars[b]	DOY	Tmax and Tmin	Lower Ter

[a] Time and duration of phenological stages of grapevine were estimated based on phenology records from South Catalonia (data not shown) and calculating accumulated a mean value of GDD needed to reach each stage at Tbase=10 ºC (Budbreak: 71 GDD; Bloom: 319 GDD; Fruitset: 429 GDD; Berry at pea size: 429 GDD; Veraison: 221 GDD; Harvest: 1857 GDD; Leaf Fall: 2163 GDD).

[b]*DOY bloom* for apples was estimated according to Funes et al. (2016)

3. Results

Results were analyzed for the baseline period (2002-2011) and for two time horizons for the RCP4.5 scenario (2020s, from 2021 to 2030, and 2040s, from 2041 to 2050). They were aggregated at three segments in each basin (upper, middle and lower basin segments; see Fig. A.2).

3.1. Climate change impacts on net hydric needs of crops

3.1.1. Current and future annual crop NHN: spatial distribution

Spatial distribution of the estimated current and future annual crop NHN in the three basins is presented in Figure 4. The highest current NHN (more than 3000 m^3/ha) are concentrated in the lower Segre (Fig. 4a) associated with maize and forage crops (from 4500-5000m^3/ha) and orchards (from 3000 to 4500 m^3/ha). In the Ter and Muga basins, higher current NHN are located in lower basin segments, mainly represented by maize, forage crops and orchards, ranging from 2000 to 4000 m^3/ha (Fig. 4b and c). In the middle and upper Muga, crops – predominantly winter cereals and olives – present current annual NHN of below 1000 m^3/ha. Crops in the middle Ter present current annual NHN of 500 to 1500 $m^{3/}$ha.

Most crops in the Segre basin are expected to experience increases in NHN (warm color ramp) with respect to the baseline (Fig. 4a) in the 2020s. These increases will stabilize or slow down in the 2040s, except for the upper course and some areas in the middle and lower basin, where NHN could decrease (cold color ramp), which explains the behavior of the total annual NHN for the whole basin (Table 5). The Ter basin presents the most variable response of crop NHN to CC of the three basins (Fig. 4b). Annual NHN could increase for most major crops in both future periods with respect to the baseline and right across the basin (warm color palette). The general trend is an increase in absolute values for the whole basin (see Table 5), except for some areas of winter cereals, for which annual NHN could decrease (cold color palette) in both periods in the lower basin, despite some recovery in the 2040s.

Crops in the Muga basin show a slight increase in their NHN (green-yellow color palette) as a response to CC from the baseline period to future periods (Fig. 4c), except for forage crops (sharp increase in NHN) and winter cereals (decrease in NHN). Forage crops show a considerable increase in the 2020s, higher than in the case of other crops (warmest colors), but since the proportion of these crops is relatively small in the Muga basin, their effect on NHN at the whole basin level is negligible; there is a much higher proportion of winter cereals, which show a decrease in NHN in the 2020s (cold colors), and this moderates the increase in all other crops, leading to a slight overall increase for the whole basin in the 2020s (Table 5).

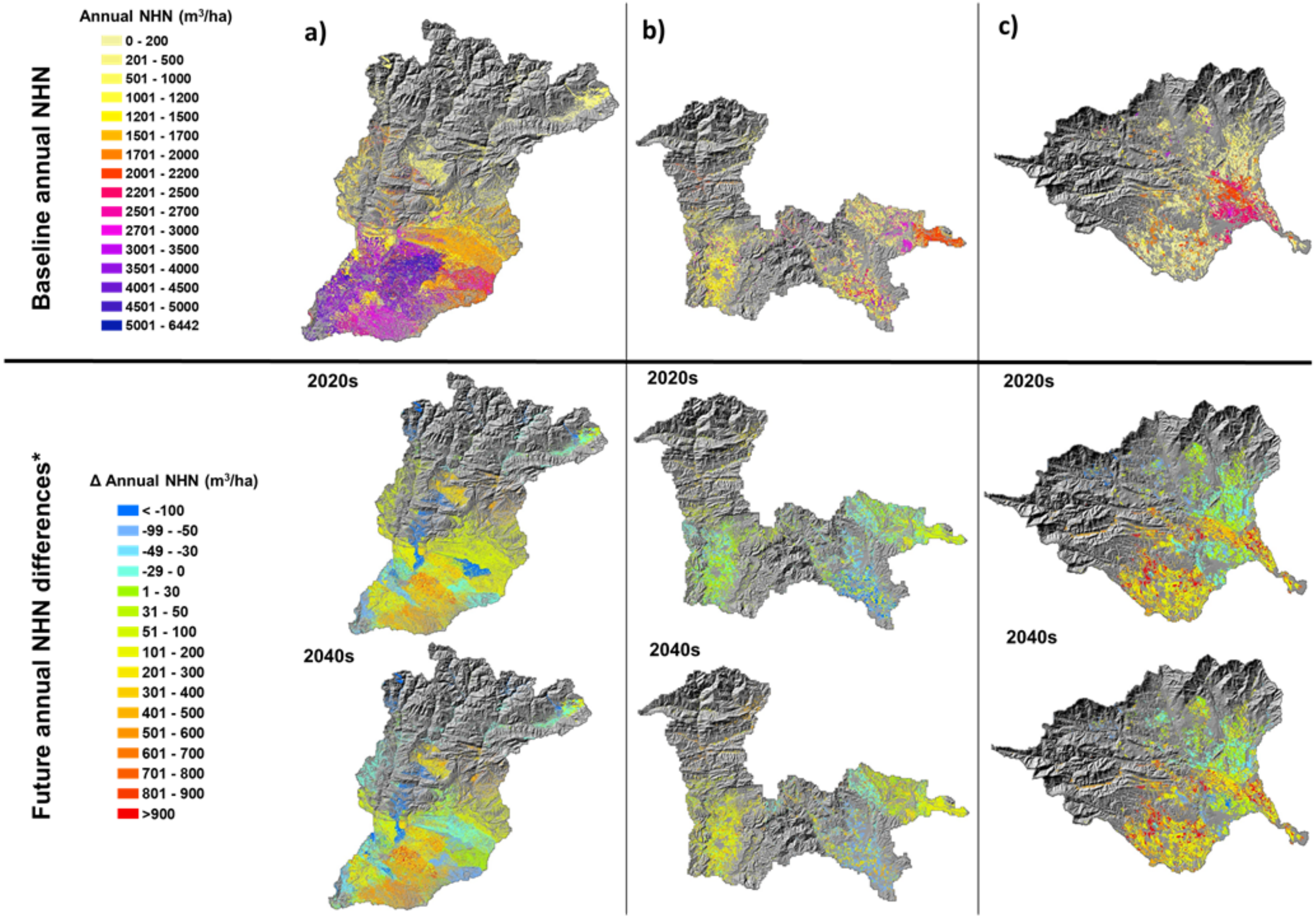

Figure 4. Spatial distribution of the annual net hydric needs (NHN) of major crops in the three case study basins (a) Segre, (b) Ter, (c) Muga in the baseline period (above), and future annual NHN differences from the baseline period at two future time periods: 2020s (2021-2030) and 2040s (2041-2050); *negative annual NHN differences imply decreases and positive differences imply increases with respect to NHN in the baseline period.

3.1.2. Current and future annual crop NHN: total basin values

Total annual NHN values in hm^3 are expected to increase for the Ter and Segre basins, although trends show different patterns in the speed and intensity of change (Table 5). In the Segre basin, the total annual increase in NHN with respect to the baseline would reach almost 53 hm^3 in the 2020s and 54 hm^3 in the 2040s, an increase of 6.6% and 6.7% respectively. In the Ter basin, the increase with respect to the baseline would be almost 1.6 hm^3 in the 2020s and 6.6 hm^3 in the 2040s, an increase of 2.5% and 10.3% respectively. As for the Muga basin, calculations show a total annual increase in NHN of almost 0.02 hm3 in the 2020s and 0.61 hm3 in the 2040s (an increase of 0.1% and 3.9% respectively), but these estimates are not statistically significant. In general, the highest increases are observed for the lower and middle basin segments, although higher relative changes (%) appear in some upper basin segments (Table 5). In the lower Segre, mean annual NHN of crops would rise from 2903 m^3/ha in the baseline to 3099 m^3/ha in the 2040s. The corresponding figures for the lower and middle Ter from the baseline to the 2040s would show an increase of almost 100 m^3/ha and 150 m^3/ha respectively. Finally, as no variation in land use or crop distribution is assumed between periods, NHN changes calculated between periods by area (m^3/ha) show the same trends and statistical significances as absolute NHN values in hm^3/year; thus, no statistically significant variation in m^3/ha between periods was obtained for the Muga basin.

Total annual NHN values (hm^3) show statistically significant differences between basin segments in all periods, with the lower course always returning the highest figures, and the upper course the lowest. The same pattern may be observed in the mean annual NHN of crops (m^3/ha) when comparing the basin segments of the Segre. However, in the Muga basin, while the upper and middle segments returned similar lower values across the different periods, the lower course showed the highest values. For its part, the Ter basin showed a gradient from the lower to the upper segment, with the middle segment presenting intermediate values not statistically different from the other two segments.

Table 5. Annual average theoretical NHN values for the total basin and lower, middle and upper basin segments (absolute values in hm^3/year and mean values in m^3/ha for the whole basin) for the baseline period (2002-2011) and both future periods under the RCP4.5 climate change scenario: 2020s (2021-2030) and 2040s (2041-2050). Differences (hm^3) and relative changes (%) in absolute NHN values of major crops with respect to the baseline period. Statistical differences in values between periods are represented with lower case letters and differences between basin segments are represented with upper case letters within each basin. Significant differences in mean values between periods and basin segments were tested by ANOVA ($p<0.05$) within each basin. No interactions were detected.

		Total Basin NHN (hm^3)	Differences* Δ hm^3 (Δ %)		Mean basin NHN (m^3/ha)		
Basin	**Basin Segment**	**Baseline**	**2020s**	**2040s**	**Baseline**	**2020s**	**2040s**
Segre	Lower basin	731.32^{Aa}	+43.01^{Ab} (+5.9)	+46.61^{b} (+6.4)	2903^{Aa}	3085^{Ab}	3099^{Ab}
	Middle basin	99.00^{Ba}	+9.92^{Bb} (+10.0)	+7.74^{Bb} (+7.8)	690^{Ba}	761^{Bb}	745^{Bb}
	Upper basin	4.98^{Ca}	-1.09^{Cb} (-21.8)	-1.10^{Cb} (-22.1)	212^{Ca}	166^{Cb}	165^{Cb}
	Whole basin	**835.30^{a}**	**+51.84^{b} (+6.2)**	**+53.25^{b} (+6.4)**	**1967^{a}**	**2097^{b}**	**2099^{b}**
Ter	Lower basin	36.2^{Aa}	+0.50^{Aab} (+1.4)	+2.80^{Ab} (+7.7)	1286^{Aa}	1302^{Aab}	1384^{Ab}
	Middle basin	24.2^{Ba}	+0.60^{Bab} (+2.5)	+2.90^{Bb} (+12.0)	1219^{ABa}	1248^{ABab}	1367^{ABb}
	Upper basin	3.6^{Ca}	+0.50^{Cab} (+13.9)	+0.80^{Cb} (+22.2)	979^{Ba}	1111^{Bab}	1207^{Bb}
	Whole basin	**64^{a}**	**+1.60^{ab} (+2.5)**	**+6.60^{b} (+10.3)**	**1239^{a}**	**1269^{ab}**	**1365^{b}**
Muga	Lower basin	10.7^{Aa}	-0.04^{Aa} (-0.4)	+0.20^{Aa} (+1.9)	1420^{Aa}	1414^{Aa}	1447^{Aa}
	Middle basin	4.6^{Ba}	+0.08^{Ba} (+1.6)	+0.41^{Ba} (+9.0)	584^{Ba}	594^{Ba}	637^{Ba}
	Upper basin	0.28^{Ca}	-0.01^{Ca} (-4.2)	-0.001^{Ca} (-0.5)	964^{Ba}	923^{Ba}	959^{Ba}
	Whole basin	**15.6^{a}**	**+0.02^{a} (+0.1)**	**+0.61^{a} (+3.9)**	**992^{a}**	**993^{a}**	**1031^{a}**

* Relative change (%) with respect to the baseline period.

3.1.3. Crop-specific current and future mean annual NHN

In the Segre, typical rainfed crops such as grapevine and almond could present an increase in their mean annual NHN in the 2040s from 9 to 15%, with olives showing an increase of up to 17% in the lower basin, where agriculture is concentrated (Table A.1). In general, winter cereals would report an increase (around 43% for barley) in the 2020s, and a subsequent slowdown in the 2040s, in accordance with the general pattern for this basin. NHN of fruit orchards such as apple would increase by up to 10% in the lower basin in the 2040s. Finally, pastures in the middle Segre would increase by up to 45% in the 2020s and almost 50% in the 2040s.

In the Ter basin, annual mean NHN of maize could increase by up to 9% and 14% in the 2040s in the lower and middle segments respectively (Table A.2). Annual NHN of ryegrass could increase by up to 11% and 15% in the 2040s in the lower and middle segments respectively, and by almost 22% in the upper segment. Winter cereals follow the same pattern in the middle and upper basin, where NHN could increase by around 10% in the 2040s. However, in the lower basin, annual NHN of winter cereals could decrease by up to 9% in the 2020s and 5% in the 2040s. Finally, in the 2020s and 2040s, annual NHN of apple trees in the lower basin could increase by around 3% and 9% respectively.

In the Muga basin, olives would consistently show an increase in NHN in the lower and middle segments, including an increase of up to 24% in the 2040s in the middle basin, where this crop is widespread (Table A.3). Grapevines would show an increase of up to 10% in the 2040s. In the same period, forage crops (alfalfa or pastures) in the middle and lower Muga could record increases with respect to the baseline of more than 8% and more than 11% (3000-4000 m^3/ha). Also in the 2040s, winter cereals such as barley could show a decrease of more than 11% and almost 23% in the middle and lower Muga respectively. Maize could see increases of almost 1% and 4% in the 2040s in the lower and middle Muga respectively.

3.1.4. Monthly crop NHN patterns

Some of the annual NHN results, such as the decrease in the annual NHN of winter cereals in several sub-basins, are easier to understand if an analysis is made of monthly behavior patterns in the NHN of crops. In general, an earlier increase in ETa in the year and a subsequent decrease for both future time horizons analyzed is observed, but it is only reflected in an increase in total annual NHN depending on crop phenology, so different monthly NHN patterns can be observed (Fig. 5). For instance, in general, in the case of orchards such as olive trees in the lower Segre, a first monthly NHN pattern can be observed: NHN only increase from May to July (Fig. 5), but no NHN increases were observed in the following summer months for future horizons with respect to the baseline (growth cycle advancement due to increased temperatures) and the annual NHN increase was modest. On the other hand, a second monthly NHN pattern for future horizons was observed in the case of forage crops, such as pastures in the middle Segre (Fig. 5): higher NHN in most of the spring and summer months, resulting in a higher annual NHN increase. Finally, a third monthly NHN pattern for future horizons may be observed in a number of crops and basin segments, such as maize in the lower Ter and barley in the lower Muga (Fig. 5): an increase in NHN in the early growing cycle balanced by lower NHN later in the cycle for phenological reasons (growth cycle advancement due to increased temperatures), resulting on occasions in an annual decrease in NHN with respect to the baseline.

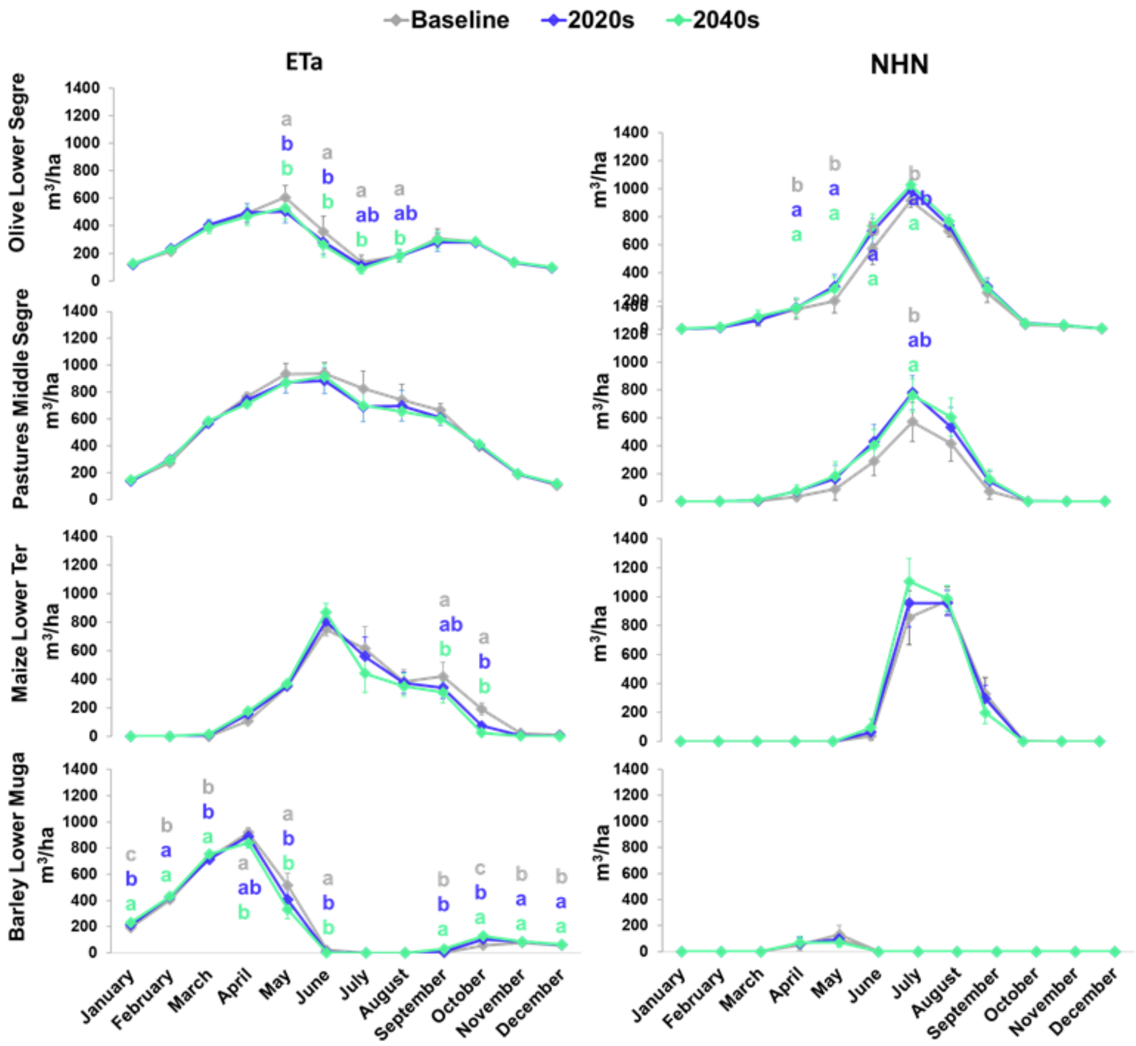

Figure 5. Patterns in monthly actual evapotranspiration (ETa, left) and net hydric needs (NHN, right): from bottom to top, barley in the lower Muga, maize in the lower Ter, pastures in the middle Segre, and olives in the lower Segre in the baseline period (2002-2011), 2020s (2021-2030) and 2040s (2041-2050). Letters represent significant differences between at least two time horizons each months. The color of the letter denotes the time horizon: gray for baseline, blue for 2020s and green for 2040s. Significant differences between mean monthly NHN values were tested by ANOVA ($p<0.05$). Time horizons with the same letter are not significantly different. An absence of letters denotes no significant differences between any time horizon.

3.2. Climate change impacts on crop growing cycle and phenology

The three patterns observed in monthly NHN in the previous section mostly reflect variations in the growing cycle determined from GDD accumulation, which produced a general advancement in the growing cycle and, depending on the species, a shortening of the cycle as well. Apart from GDD accumulation, several general agroclimatic indices calculated show this, but the specific growing cycle indices estimated for several species (maize, grapevine and apple) also show changes in their respective growing cycles.

Frost days in March and April would decrease throughout the three basins, most markedly in the upper and middle basin segments (Table 6). This does not necessarily mean a reduction or disappearance of frost risk because of the advancement of the crop cycle, as can be seen in *DOYT10*, which indicates an advancement of the growing cycle of up to 8-12, 7-10 or 5-8 days in the lower, middle and upper basin, respectively, in the 2040s. The number of days with risk of heat damage in July and August would increase in all basins and segments (Table 6). *Heat 30 days* shows an increase of 3-5 days in the 2040s depending on the basin and the segment, except in the upper Segre where the increase in the 2040s is barely 1 day. *Heat 35 days* would approximately double in all basins in the 2040s in relation to the baseline.

Both maize-specific indicators related to the rapid completion of the growing cycle (*DOY 600FAO* and *DOY700FAO,* Table 6) show that it could be shortened in the 2040s compared to the baseline, ranging from 20 to 27 days shorter, depending on the basin and segment. For grapevine, DOY pheno at budbreak would be reached 7 days earlier in the 2020s and 10 days earlier in the 2040s compared to the baseline (Figure A.6 of Appendix A), while*Days pheno* to harvest after budbreak (180 days in the baseline period) would be shortened by up to 6 days in the 2020s and 11 days in the 2040s, mainly due to shortening in all phases after blooming, particularly from veraison to harvest. Although *Days pheno* at the blooming phase would last up to 6 days longer in the 2040s, *DOY pheno* at blooming would be slightly advanced because of earlier budbreak. Finally, the shortening of the growing cycle would result in an earlier *DOY pheno* at harvest of about 13 days in the 2020s and 21 days in the 2040s. DOY bloom in apples would show no changes in the 2020s or 2040s: in spite of a delay at the beginning of chill accumulation of almost 10 days, an equivalent, counterbalancing effect is observed during the heat accumulation phase, and no changes would occur during the chilling phase (Fig. A.7 of Appendix A).

Table 6. General and maize-specific indicators for growth and development in the upper, middle and lower segments of the case study basins for baseline (2002-2011) and future periods (2020s and 2040s) under the RCP 4.5 scenario. The definition of each indicator can be found in Table 4.

			Segre									Ter									Muga								
			Upper			Middle			Lower			Upper			Middle			Lower			Upper			Middle			Lower		
	Indicator		Baseline	Δ2020s	Δ2040s	Baseline	Δ2020s	Δ2040s	Baseline	Δ2020s	Δ2040s	Baseline	Δ2020s	Δ2040s	Baseline	Δ2020s	Δ2040s	Baseline	Δ2020s	Δ2040s	Baseline	Δ2020s	Δ2040s	Baseline	Δ2020s	Δ2040s	Baseline	Δ2020s	Δ2040s
General indicators	Frost days	March	19.6	-0.5	-1.4	13.3	-0.6	-1.8	5.4	-0.4	-1.5	17.3	-1.3	-2.3	7.8	-0.8	-1.9	6.5	-0.3	-0.9	8.4	-1.1	-2.1	2.7	-0.1	-0.1	1.7	-0.1	-0.4
		April	19.6	-7.8	-8.7	4.6	-0.5	-1.1	0.4	-0.1	-0.2	7.1	-1.1	-1.7	0.8	-0.1	-0.5	0.5	-0.1	-0.3	1	-0.6	-0.3	0	0	0	0	0	0
	Heat 30 days	July	0.7	+0.6	+0.9	13.6	+2.9	+5	22.1	+2.7	+4	4.4	+2.8	+5.0	14.1	+2.8	+4.8	17.6	+1.6	+3.0	9	+2.1	+3.9	12.9	+1.9	+3.9	13.8	+2.7	+3.9
		August	0.7	+0.5	+0.9	11.5	+2.8	+4.8	19.2	+3.1	+4.4	3.5	+2.4	+4.5	10.6	+2.8	+5	15.3	+2	+4	5.5	+1.8	+3.8	11	+2.3	+4.7	11.8	+2.7	+4.6
	Heat 35 days	July	0	0	0	2.4	+1.5	+3.2	5.1	+3.3	+5.6	0	+0.3	+0.4	1.2	+1	+1.9	2.8	+1.2	+2.4	0.4	+0.4	+0.9	0.5	+0.5	+0.9	1.2	+0.4	+1
		August	0	0	0	2.4	+1	+2.5	4.2	+1.9	+3.8	0.3	+0.3	+0.6	1.5	+0.6	+1.5	3.7	+0.7	+1.9	0.5	+0.4	+0.6	1.3	+0.2	+0.7	1	+0.8	+1.5
	DOY T10		150	-2	-5	108	-3	-7	82	-4	-10	131	-4	-8	101	-4	-7	80	-1	-8	107	0	-5	79	-4	-10	70	-7	-12
Maize indicators	DOY 600FAO		†	†	†	‡	‡	‡	282	-13	-22	†	†	†	‡	‡	‡	299	-14	-24	†	†	†	299	-11	-23	284	-14	-23
	DOY 700FAO		†	†	†	‡	‡	‡	285	-11	-20	†	†	†	‡	‡	‡	307	-19	-27	†	†	†	303	-8	-20	289	-13	-22

† *Maize is not a major crop in this basin segment, so calculations were not performed.*

‡ *Calculations were not performed as the required GDD are not attained in all years in most of the sub-basins, at least in the reference period.*

4. Discussion

Our estimations showed the main impacts of CC on the NHN, growing cycle and phenology of major crops in three Mediterranean basins in the first half of the 21st century under the RCP4.5 scenario, a GHGs emission stabilization scenario that assumes the execution of mitigation policies (Thomson et al., 2011).

4.1. Projected changes in the NHN of crops

Most crops in the three basins could experience a significant increase in NHN until mid-century with respect to the baseline period (Fig. 4; Table A.1 to A.2 and Table 5), as shown by similar studies under Mediterranean (Phogat et al., 2018; Zhao et al., 2015; Valverde et al., 2015; Savé et al., 2012; see review in Iglesias and Garrote, 2015) and non-Mediterranean conditions (Hong et al., 2016; see review in Iglesias and Garrote, 2015; McDonald and Girvetz, 2013). However, NHN decreases have been calculated for some crops (especially for winter cereals) at certain locations in all the case study basins up until 2050 under the RCP4.5 scenario. Although NHN decreases are also projected in other studies (Hong et al., 2016; Zhao et al., 2015; Lorite et al., 2018), this is not an obvious result. These decreases are associated with changes in duration (shortening) or beginning (advancement) of the growing cycle, particularly in annual crops (Fig. A.6). Shortening and advancement of the growing cycle partially compensates or overcompensates the earlier NHN increase in some annual crops. A shortened and advanced growing cycle leads to a lower demand for water due to higher soil water availability, and there is also less time for water to be consumed. We believe there are two main reasons for these novel results: first, they were obtained under the RCP4.5 scenario, a pathway for stabilization of radiative forcing by 2100 (IPCC 2014) in contrast with the A2 scenario from AR4; and secondly, we were able to fine-tune our calculations by using homogeneous climate, crop type and soil type units, which leads to more reliable estimations of ETa. The reason we were able to arrive at these fine-tuned results is that our study is one of the few that considers general and exhaustively projected changes in the NHN of major crops at a basin scale, including the range of conditions of a specific region.

In general and in terms of absolute values, NHN would increase in the Ter and Segre basins, albeit in a different way, throughout the first half of the century. NHN increases range from small to moderate in the 2020s to moderate to high in the 2040s. Dynamics would vary for the three basins: there would be no statistically significant variation for the Muga basin a continuous increase for the Ter basin, and an initial increase followed by stability in the Segre basin (Table 5). These general trends vary from crop to crop (Table A.1 to A.3). The highest increases in NHN are found in the lower segments of the basins, where agriculture is spatially concentrated (Table 5). Most notably, in the lower Segre annual NHN (total values) would increase by 43.7 and 47 hm^3/year in the 2020s and 2040s respectively. Lower annual NHN increases (total values) are estimated the lower Ter: 2.8 hm^3/year in the 2040s.

At all events, a generalized increase in NHN is observed in the case study basins; combined with lower water availability, which restricts irrigation, this could become very limiting for crop production.

4.2. Projected changes and impacts on crop growing cycle and phenology

A general advancement of the crop growing cycle has been shown throughout the future time horizons in this study. Moreover, a shortened crop growing cycle has been estimated in annual crops such as maize (Table 6) and temperate fruits such as grapevine (Fig. A.6). However, a general prolongation of the vegetative season was predicted by some authors (Trnka et al., 2011; Tian et al., 2014), opening new time windows for cropping. The behavior of some herbaceous crops such as pastures (Fig. 5) fit this pattern. A higher number of days presenting extremely hot temperature (*Heat 30 days* and *Heat 35 days*) as projected for the three basins (Table 6) is consistent with the current increase in detrimental heat effects in the study area, such as the heat stroke observed in apple (Joaquim Carbó, personal communication), seriously affecting fruit quality. A decrease in *Frost days* (Table 6) would not necessarily mean a reduction or disappearance of frost risk. In fact, the projected advancement and shortening of the crop growing cycle could counterbalance this reduction in frost days, leading to an increase in spring frost risk (Darbyshire et al., 2013), as early phenological stages may still occur when frost events are still frequent despite the advancement of the crop growing cycle. These changes (Table 6; Fig. A.6 and A.7) are in line with other studies that assess crop growing cycle and phenology (Trnka et al., 2011; Saadi et al., 2015; Ruiz-Ramos et al., 2018; Koufos et al., 2018).

Upper segments of basins would experience the greatest climatic changes, because they are the coldest and wettest. However, effects on crop production would be higher in the middle and lowest segments of basins since this is where most of the cropland is situated. The coastal effect leads to clear differences between the lower basin and the rest of the basin, except in the case of the Segre, as this is a tributary river and its lower course is clearly inland.

4.3. Adaptation measures and strategies

Adaptation measures and strategies should be consistent with the results presented so far, in order to reduce the future impacts of CC and facilitate the design of more resilient agricultural water management systems in Catalonia as a whole. These measures would mainly consist in: i) Changing the water management scheme; ii) changing the crop distribution and crop choices (low water demand crops; Allain et al., 2018; Mo et al., 2017; Ronco et al., 2017); iii) Applying support or supplementary irrigation and increasing irrigation efficiency (Ruiz-Ramos et al., 2018; Dechmi and Skhiri, 2013); iv) Adjusting irrigation to net irrigation requirements (Dechmi and Skhiri, 2013; Allain et al., 2018; Pascual et al., 2018); v)

Adjusting sowing dates and the cropping calendar (Rotter et al., 2013; Ruiz-Ramos et al., 2017); and vi) Changing to cultivars or crops more suited to adverse conditions (Mo et al., 2017; Ronco et al., 2017). These measures would also form part of a water management strategy: in line with our results, some research in the study area (Milano et al., 2013 in the Ebro basin and Vicente-Serrano et al., 2017a in the Segre basin) has concluded that a future scenario characterized by higher demands together with decreased water availability is highly plausible. Therefore, it will be necessary to adopt new water use and management strategies in the case study basins in order to maintain yields and improve agriculture. For example, beyond increasing irrigation efficiency, adjusting irrigation to hydric needs and not to a predetermined concession should form part of a water management strategy in a water and land governance framework; the decision to use low water demand crops or varieties should not simply be left to the growers, but it should also be included in a water governance scheme, together with restricting the area of higher water consuming crops or defining support irrigation protocols to allow crop survival in the driest years.

In fact, many other adaptation measures and strategies could be proposed, such as the following: a shift in diet towards a reduction in meat consumption, since fodder crops are large water and land consumers (Vanham et al. 2016); changes in land use and forest management to regulate water availability for the basin (Zabalza-Martínez et al., 2018); rainwater harvesting and storage (Rockström, 2002); reuse of wastewater in agriculture (Panagopoulos et al, 2014; Ronco et al., 2017); crop diversification and crop rotation by alternating water-demanding crops with crops that demand less water (Allain et al., 2018; Lin, 2011); and conservation agriculture (Prestele et al., 2018) or physically protecting crops from adverse events by establishing abatement infrastructures. Clearly, some of these measures would also form part of a water management scheme.

As a matter of fact, choosing site-specific measures and combining them are the most appropriate options when seeking to adapt agricultural systems to CC measures (Dechmi and Skhiri, 2013; Ruiz-Ramos et al., 2017). Moreover, the implementation of policies, including water management, with a combination of CC mitigation and adaptation measures is highly recommended in order to make agricultural systems more resilient and obtain high yields (FAO, 2013).

4.4. Limitations of the study

Due to the methodology used in this study for NHN estimations based on Savé et al., (2012), some limitations must be acknowledged that make it necessary to look at our results with some care, although we believe the effect of these limitations is negligible. First, although no uncertainty or validation analyses have been performed, similar annual ETc and NHN values (estimated for the baseline period) were obtained for maize and apple trees in GIROREG experiences (from 2014 to 2017) in the Muga and Ter basins within the framework of LIFE MEDACC (Francesc Camps, personal communication). Similar values of annual NHN for wheat have been reported by Saadi et al., (2015): 275 mm in the area of Lleida compared with 211.6 mm estimated in the present study for the lower Segre (Table A. 1).

Secondly, the delta method used in climate projections will probably not reflect extreme values. However, intra-annual variability is already considered in the projections by using different deltas for the different seasons; and, as projections are applied to mean values for long periods (more than 10 years), interannual variability is not the main focus, also because uncertainty in extreme values is much greater than in mean values.

Thirdly, the effect on crop transpiration of increased CO_2 in the RCP 4.5 scenario was not considered in the NHN calculation. Some authors (Elliot et al., 2014, Zhao et al., 2015) have highlighted the importance of considering increased CO_2. However, following the arguments presented by Savé et al. (2012), we thought that the uncertainties of not considering increased CO_2 effects would motivate a correction of our results, but we do not believe these corrections would raise or lower the estimations presented here. First of all, the CO_2 increase in the RCP4.5 scenario is very small, so no substancialtrffg0744 reductions in stomatal conductance are to be expected, and this reduction would be partially compensated by a higher leaf area index, also resulting from plant adaptation to higher CO_2 concentrations, giving a similar transpiration per soil area.

Fourthly, another source of uncertainty can be found in the use of estimated soil maps for the case study basins, as soil attributes such as available water capacity are determinant for crop NHN estimation through estimation of ETa. However, no complete high-resolution soil maps were available for the study area.

Fifthly, estimations based on phenological and agroclimatic models that are valid in the reference period are implicitly assumed to be valid for the estimated periods. Moreover, the estimated changes in growing cycle in this study are based on GDD accumulation, and changes in phenology for grapevines or maize use very simple models also based on GDD accumulation.

Finally, the health status of the crop would undoubtedly affect these results, and pests and diseases are expected to increase in the Mediterranean as a result of climate change (MedECC 2019).

Beyond this, crop performance will be affected by agronomical practices, local edaphic conditions and production needs, i.e. the market, which have not been included in the calculations. Moreover, this study has focused on the expected conditions for current crops in the basins where they are now being grown: based on the results in this study, conclusions could be drawn about the degree of productivity of these crops in their present locations.

4.5. Recommendations and future work

Integrating the results of this study with hydrological modeling for future climate and land use scenarios would make it possible to estimate the gap (the deficit or imbalance) between water supply and water demands with regard to agriculture in the area and to design water management strategies.

Moreover, further modeling work becomes necessary for the purpose of simulating different initiatives and/or scenarios (concerning water management, land use changes, best management practices in agriculture and CC scenarios) at the basin or regional scale, in order to test different adaptation and mitigation strategies for Catalonia.

5. Conclusion

Most crops in the case study basins would show significant NHN increases before mid-century, directly related with increased crop potential evapotranspiration and decreased precipitation during the growing season. The generalized NHN increase and the low water availability for irrigation could challenge the feasibility of maintaining the current agricultural model in the study area. Other key results of this work are a general advancement and shortening of the growing cycle, lengthening of the vegetating season, impacts on phenology and damages associated with extreme temperatures. These future scenarios open up new possibilities in terms of crop and variety choices, adjustment of the cropping calendar and a wide range of CC adaptation measures that should form part of any water management scheme within a governance framework. This study represents a starting point from which to simulate adaptation and mitigation strategies that will be instrumental in the design of more resilient agricultural systems in Catalonia, including water management, and its findings could be partially extrapolated to many other regions of the Mediterranean basin.

Acknowledgements

This work was supported by the research project “LIFE12 ENV/ES/000536-Demonstration and validation of innovative methodology for regional climate change adaptation in the Mediterranean area (LIFE MEDACC)”, financed by the LIFE program of the European Commission. We would like to thank the Coordination service for registration and financial aid of the Ministry of Agriculture, Livestock, Fisheries and Food (Government of Catalonia) for data on the declaration of eligible agricultural areas for common Agricultural Policy payments for the year 2013. Finally, we want to thank the reviewers for their constructive comments and Sergio Vicente (IPE-CSIC) for his work on climate projections and his suport in the review process.

Appendix A and B. Supplementary material and more methodological details.

Supplementary data associated with this article can be found in the online version at doi:10.1016/j.agwat.2021.106797.

References

1. ACA, IRTA. (2008). Pla per a l’eficiencia en l’ús de l’aigua per a reg agrícola. Agencia Catalana de l’aigua i Institut de recerca i tecnología agroalimentaria.
2. Allain, S., Ndong, G. O., Lardy, R., and Leenhardt, D. (2018). Integrated assessment of four strategies for solving water imbalance in an agricultural landscape. Agronomy for Sustainable Development 38, 12.
3. Allen, R.G., Pereira, L.S., Raes, D., Smith, M. (1998). Crop evapotranspiration — guidelines for computing crop water requirements. FAO Irrigation and drainage paper 56. Food and Agriculture Organization, Rome.

4. Arnold J.G., Srinivasan R., Muttiah R.S., Williams J.R. (1998). Large-area hydrologic modeling and assessment: Part I. Model development. Journal American Water Resources Association, 34(1), 73-89.

5. Caubel, J., García de Cortázar-Atauri, I., Launay, M., de Noblet-Ducoudré, N., Huard, F., Bertuzzi, P., and Graux, A.I. (2015). Broadening the scope for ecoclimatic indicators to assess crop climate suitability according to ecophysiological, technical and quality criteria. Agricultural and Forest Meteorology 207, 94-106.

6. Clarke D. (1998). CROPWAT for Windows: User Guide. FAO, Rome.

7. Connor, J. D., Schwabe, K., King, D., and Knapp, K. (2012). Irrigated agriculture and climate change: The influence of water supply variability and salinity on adaptation. Ecological Economics 77, 149-157.

8. Cramer, W., Joel, G., Fader, M., Garrabou, J., Gattuso, J.-P., Iglesias, A., A. Lange, M., Lionello, P., Carmen Llasat, M., Paz, S., Peñuelas, J., Snoussi, M., Toreti, A., N. Tsimplis, M., and Xoplaki, E. (2018). "Climate change and interconnected risks to sustainable development in the Mediterranean."

9. Darbyshire, R., Webb, L., Goodwin, I., and Barlow, E. W. (2013). Evaluation of recent trends in Australian pome fruit spring phenology. Int J Biometeorol 57, 409-21.

10. Dechmi, F., and Skhiri, A. (2013). Evaluation of best management practices under intensive irrigation using SWAT model. Agricultural Water Management 123, 55-64.

11. DUN. (2013). Declaration of eligible agricultural area for Common Agricultural Policy payments. Government of Catalonia. Annual

12. Elliott, J., Deryng, D., Müller, C., Frieler, K., Konzmann, M., Gerten, D., Glotter, M., Flörke, M., Wada, Y., Best, N., Eisner, S., Fekete, B. M., Folberth, C., Foster, I., Gosling, S. N., Haddeland, I., Khabarov, N., Ludwig, F., Masaki, Y., Olin, S., Rosenzweig, C., Ruane, A.

C., Satoh, Y., Schmid, E., Stacke, T., Tang, Q., and Wisser, D. (2014). Constraints and potentials of future irrigation water availability on agricultural production under climate change. Proceedings of the National Academy of Sciences 111, 3239-3244.

13. FAO. (2013). Sourcebook on Climate Smart Agriculture, Forestry and Fisheries, Food and Agriculture Organization of the United Nations (FAO), Rome, Italy. http://www.fao.org/climatechange/37491-0c425f2caa2f5e6f3b9162d39c8507fa3.pdf

14. Funes, I., Aranda, X., Biel, C., Carbo, J., Camps, F., Molina, A. J., de Herralde, F., Grau, B., and Save, R. (2016). Future climate change impacts on apple flowering date in a Mediterranean subbasin. Agricultural Water Management 164, 19-27.

15. Girard, C., Pulido-Velazquez, M., Rinaudo, J. D., Page, C., and Caballero, Y. (2015). Integrating top-down and bottom-up approaches to design global change adaptation at the river basin scale. Global Environmental Change-Human and Policy Dimensions 34, 132-146.

16. Girona, J., Marsal, J., Mata, M., del Campo, J. (2004). Pear crop coefficients obtained in a large weighing lysimeter. In Proceedings of the IVth International Symposium on Irrigation of Horticultural Crops, Snyder, R. L., Ed. Int Soc Horticultural Science: Leuven 1; pp 277-281.

17. Girona J., del Campo J., Mata M., Lopez G., Marsal J. (2011) A comparative study of apple and pear tree water consumption measured with two weighing lysimeters. Irrigation Science 29: 55-63.

18. Hong, E. M., Nam, W. H., Choi, J. Y., and Pachepsky, Y. A. (2016). Projected irrigation requirements for upland crops using soil moisture model under climate change in South Korea. Agricultural Water Management 165, 163-180.

19. ICC, (2012). Digital elevation model (30 m resolution). Institut Cartogràfic de Catalunya, 2012 [online].

20. Iglesias, A., and Garrote, L. (2015). Adaptation strategies for agricultural water management under climate change in Europe. Agricultural Water Management 155, 113-124.

21. IPCC. (2014). Climate Change 2014: Synthesis Report. Contribution of Working Groups I, II and III to the Fifth Assessment Report of the Intergovermmental Panel on Climate Change [Core Writing Team, R.K. Pachauri and L.A. Meyer (eds.)].IPCC, Geneva, Switzerland, 151 pp. https://www.ipcc.ch/reports/

22. Koufos, G. C., Mavromatis, T., Koundouras, S., and Jones, G. V. (2018). Response of viticulture-related climatic indices and zoning to historical and future climate conditions in Greece. International Journal of Climatology 38, 2097-2111.

23. Licciardello, F., G. Rossi, C., Srinivasan, R., M. Zimbone, S., and Barbagallo, S. (2011). Hydrologic Evaluation of a Mediterranean Watershed Using the SWAT Model with Multiple PET Estimation Methods. Transactions of the ASABE 54, 1615-1625.

24. Lin, B. B. (2011). Resilience in Agriculture through Crop Diversification: Adaptive Management for Environmental Change. BioScience 61, 183-193.

25. Lorite, I. J., Gabaldón-Leal, C., Ruiz-Ramos, M., Belaj, A., de la Rosa, R., León, L., and Santos, C. (2018). Evaluation of olive response and adaptation strategies to climate change under semi-arid conditions. Agricultural Water Management 204, 247-261.

26. Marsal J., Girona J., Casadesus J., Lopez G., Stöckle C.O. (2013). Crop coefficient (Kc) for apple: comparison between measurements by a weighing lysimeter and prediction by CropSyst. Irrigation Science, 31:455–463. DOI 10.1007/s00271-012-0323-7.

27. Marsal, J., Casadesus, J., Lopez, G., Mata, M., Bellvert, J., and, Girona, J. (2016). Sustainability of regulated deficit irrigation in a mid-maturing peach cultivar. Irrigation Science 34, 201-208.

28. McDonald, R. I., and Girvetz, E. H. (2013). Two Challenges for U.S. Irrigation Due to Climate Change: Increasing Irrigated Area in Wet States and Increasing Irrigation Rates in Dry States. PLOS ONE 8, e65589.

29. MedECC. First Mediterranean Report MedECC (2019; https://www.medecc.org/wp-content/uploads/2018/12/MedECC-Booklet_EN_WEB.pdf).

30. Milano, M., Ruelland, D., Dezetter, A., Fabre, J., Ardoin-Bardin, S., and Servat, E. (2013). Modeling the current and future capacity of water resources to meet water demands in the Ebro basin. Journal of Hydrology 500, 114-126.

31. Mo, X.-G., Hu, S., Lin, Z.-H., Liu, S.-X., and Xia, J. (2017). Impacts of climate change on agricultural water resources and adaptation on the North China Plain. Advances in Climate Change Research 8, 93-98.

32. Neitsch, S.L., Arnold, J.G., Kiniry, J.R. and Williams, J.R. (2005). Soil and Water Assessment Tool (SWAT) Theoretical Documentation. Blackland Research Center, Texas Agricultural Experiment Station and Grassland, Soil and Water Research Laboratory, Temple, TX.

33. Neitsch, S. L., Arnold, J. G., Kiniry, J. R., Srinivasan, R., and Williams, J. R. (2011). Soil and Water Assessment Tool Input/Output File Documentation: Version 2009, Texas Water Resources Institute Technical Report 365, Texas A&M University System, College Station (Texas).

34. Olesen, J. E., and Bindi, M. (2002). Consequences of climate change for European agricultural productivity, land use and policy. European Journal of Agronomy 16, 239-262.

35. Panagopoulos, Y., Makropoulos, C., Kossida, M., and Mimikou, M. (2014). Optimal Implementation of Irrigation Practices: Cost-Effective Desertification Action Plan for the Pinios Basin. Journal of Water Resources Planning and Management 140, 05014005.

36. Pascual, D., Pla, E., Lopez-Bustins, J. A., Retana, J., and Terradas, J. (2015). Impacts of climate change on water resources in the Mediterranean Basin: a case study in Catalonia, Spain. Hydrological Sciences Journal-Journal Des Sciences Hydrologiques 60, 2132-2147.

37. Pascual D., Zabalza Martinez J., Funes I., Vicente-Serrano S.M., Pla E., Savé R., Aranda X., Biel C. (2016). Methodology to assess climate change impacts in the LIFE MEDACC case-study basins: Generation of scenarios, vulnerability maps and quantification of impacts. Deliverable 13. LIFE MEDACC. http://medacc-life.eu/sites/medacc-life.eu/files/docuemnts/d13_methodologyseriesmaps_v4.pdf

38. Pascual D., Pla E., Zabalza Martinez J., Vicente-Serrano S.M., Funes I., Savé R., Aranda X., Biel C. (2018). Effects of the implementation actions in LIFE MEDACC case study basins. Deliverable 22. LIFE MEDACC. http://medacc-life.eu/sites/medacc-life.eu/files/docuemnts/d22_monitoringresults_7.pdf

39. Phogat, V., Cox, J. W., and Simunek, J. (2018). Identifying the future water and salinity risks to irrigated viticulture in the Murray-Darling Basin, South Australia. Agricultural Water Management 201, 107-117.

40. Prestele, R., Hirsch, A. L., Davin, E. L., Seneviratne, S. I., and Verburg, P. H. (2018). A spatially explicit representation of conservation agriculture for application in global change studies. Global Change Biology 24, 4038-4053.

41. Rockstrom, J. (2000). Water resources management in smallholder farms in Eastern and Southern Africa: An overview. Physics and Chemistry of the Earth, Part B: Hydrology, Oceans and Atmosphere 25, 275-283.

42. Ronco, P., Zennaro, F., Torresan, S., Critto, A., Santini, M., Trabucco, A., Zollo, A. L., Galluccio, G., and Marcomini, A. (2017). A risk assessment framework for irrigated agriculture under climate change. Advances in Water Resources 110, 562-578.

43. Rötter, R. P., Höhn, J., Trnka, M., Fronzek, S., Carter, T. R., and Kahiluoto, H. (2013). Modelling shifts in agroclimate and crop cultivar response under climate change. Ecology and Evolution 3, 4197-4214.

44. Ruiz-Ramos, M., Ferrise, R., Rodriguez, A., Lorite, I. J., Bindi, M., Carter, T. R., Fronzek, S., Palosuo, T., Pirttioja, N., Baranowski, P., Buis, S., Cammarano, D., Chen, Y., Dumont, B., Ewert, F., Gaiser, T., Hlavinka, P., Hoffmann, H., Hohn, J. G., Jurecka, F., Kersebaum, K. C., Krzyszczak, J., Lana, M., Mechiche-Alami, A., Minet, J., Montesino, M., Nendel, C., Porter, J. R., Ruget, F., Semenov, M. A., Steinmetz, Z., Stratonovitch, P., Supit, I., Tao, F., Trnka, M., de Wit, A., and Rotter, R. P. (2018). Adaptation response surfaces for managing wheat under perturbed climate and CO2 in a Mediterranean environment. Agricultural Systems 159, 260-274.

45. Saadi, S., Todorovic, M., Tanasijevic, L., Pereira, L. S., Pizzigalli, C., and Lionello, P. (2015). Climate change and Mediterranean agriculture: Impacts on winter wheat and tomato crop evapotranspiration, irrigation requirements and yield. Agricultural Water Management 147, 103-115.

46. Savé, R., de Herralde, F., Aranda, X., Pla, E., Pascual, D., Funes, I., and Biel, C. (2012). Potential changes in irrigation requirements and phenology of maize, apple trees and alfalfa under global change conditions in Fluvia watershed during XXIst century: Results from a modeling approximation to watershed-level water balance. Agricultural Water Management 114, 78-87.

47. SIGPAC. (2013). Agricultural Plots Geographical Information System. Government of Catalonia. Shapefile. Annual

48. Thomson, A. M., Calvin, K. V., Smith, S. J., Kyle, G. P., Volke, A., Patel, P., Delgado-Arias, S., Bond-Lamberty, B., Wise, M. A., Clarke, L. E., and Edmonds, J. A. (2011).

RCP4.5: a pathway for stabilization of radiative forcing by 2100. Climatic Change 109, 77.

49. Tian, Z., Yang, X., Sun, L., Fischer, G., Liang, Z., and Pan, J. (2014). Agroclimatic conditions in China under climate change scenarios projected from regional climate models. International Journal of Climatology 34, 2988-3000.

50. TICCC. Government of Catalonia; Institute of Catalan Studies. (2016). Climate change in Catalonia: Executive summary of the Third Report on Climate Change in Catalonia. Writing team: Xavier Duran, M. Josep Picó and Lluís Reales. Edited by Arnau Queralt, Barcelona. Available online at: http://cads.gencat.cat/ca/detalls/detallarticle/Tercer-informe-sobre-el-canvi-climatic-a-Catalunya-00003

51. Trnka, M., Eitzinger, J., Semerádová, D., Hlavinka, P., Balek, J., Dubrovský, M., Kubu, G., Štěpánek, P., Thaler, S., Možný, M., and Žalud, Z. (2011). Expected changes in agroclimatic conditions in Central Europe. Climatic Change 108, 261-289.

52. Valverde, P., Serralheiro, R., de Carvalho, M., Maia, R., Oliveira, B., and Ramos, V. (2015). Climate change impacts on irrigated agriculture in the Guadiana river basin (Portugal). Agricultural Water Management 152, 17-30.

53. Vanham, D., del Pozo, S., Pekcan, A. G., Keinan-Boker, L., Trichopoulou, A., and Gawlik, B. M. (2016). Water consumption related to different diets in Mediterranean cities. Science of the Total Environment 573, 96-105.

54. Vicente-Serrano S. M., Zabalza J., Pla E., Pascual D., Serrano R., Borràs G., Savé R., Biel C. (2014). Protocol of database quality and homogeneity. Deliverable 4. Life-MEDACC.http://medacc-life.eu/sites/medacc-life.eu/files/docuemnts/deliverable_4_life_medacc.pdf

55. Vicente-Serrano, S. M., Zabalza-Martinez, J., Borras, G., Lopez-Moreno, J. I., Pla, E., Pascual, D., Save, R., Biel, C., Funes, I., Azorin-Molina, C., Sanchez-Lorenzo, A., Martin-

Hernandez, N., Pena-Gallardo, M., Alonso-Gonzalez, E., Tomas-Burguera, M., and El Kenawy, A. (2017a). Extreme hydrological events and the influence of reservoirs in a highly regulated river basin of northeastern Spain. Journal of Hydrology-Regional Studies 12, 13-32.

56. Vicente-Serrano, S. M., Zabalza-Martinez, J., Borras, G., Lopez-Moreno, J. I., Pla, E., Pascual, D., Save, R., Biel, C., Funes, I., Martin-Hernandez, N., Pena-Gallardo, M., Begueria, S., and Tomas-Burguera, M. (2017b). Effect of reservoirs on streamflow and river regimes in a heavily regulated river basin of Northeast Spain. Catena 149, 727-741.

57. Zabalza-Martínez, J., Vicente-Serrano, S., López-Moreno, J., Borràs Calvo, G., Savé, R., Pascual, D., Pla, E., Morán-Tejeda, E., Domínguez-Castro, F., and Tague, C. (2018). The Influence of Climate and Land-Cover Scenarios on Dam Management Strategies in a High Water Pressure Catchment in Northeast Spain. Water 10, 1668.

58. Zahn, M.; von Storch, H. (2010). Decreased frequency of North Atlantic polar lows associated with future climate warming. Nature 467, 309.

59. Zhao, G., Webber, H., Hoffmann, H., Wolf, J., Siebert, S., and Ewert, F. (2015). The implication of irrigation in climate change impact assessment: a European-wide study. Global Change Biology 21, 4031-4048.